$\mu \to e\gamma$ in a supersymmetric radiative neutrino mass model

Raghavendra Srikanth Hundi
Department of Physics,
Indian Institute of Technology Hyderabad,
Kandi, Sangareddy - 502 285, Telangana, India.

E-mail: rshundi@iith.ac.in

arXiv:1510.02253v2 [hep-ph] 21 Dec 2015

Abstract

We have considered a supersymmetric version of the inert Higgs doublet model, whose motivation is to explain smallness of neutrino masses and existence of dark matter. In this supersymmetric model, due to the presence of discrete symmetries, neutrinos acquire masses at loop level. After computing these neutrino masses, in order to fit the neutrino oscillation data, we have shown that by tuning some supersymmetry breaking soft parameters of the model, neutrino Yukawa couplings can be unsuppressed. In the above mentioned parameter space, we have computed branching ratio of the decay $\mu \to e\gamma$. To be consistent with the current experimental upper bound on $Br(\mu \to e\gamma)$, we have obtained constraints on the right-handed neutrino mass of this model.

PACS numbers: 12.60.Jv, 13.35.Bv, 14.60.Pq

1 Introduction

There are many indications for physics beyond the standard model (SM) [1]. One among them is the existence of non-zero neutrino masses [2]. Some of the indications for new physics can be sucessfully explained in supersymmtric models [3]. For this reason, neutrino masses have been addressed in supersymmetry. In a neutrino mass model, there is a possibility for lepton flavor violation (LFV) [4], for which there is no direct evidence. Experiments have put upper bounds on the branching ratios of these LFV processes [5, 6, 7]. Due to Glashow-Iliopoulos-Maiani cancellation mechanism, these processes are highly suppressed in the SM and the above mentioned upper bounds are obviously satisfied in it. However, a signal for any LFV process with an appreciable branching ratio gives a confirmation for new physics.

In this work, we study LFV processes of the form $\ell_i \to \ell_j \gamma$ in a supersymmetrized model for neutrino masses [8]. Here, $\ell_i, i = 1, 2, 3$, are charged leptons. The above mentioned model arises after supersymmetrizing the inert Higgs doublet model [9, 10]. The inert Higgs doublet model [9] offers explanation for neutrino masses and dark matter. In this model [9], dark matter is stable due to an exact Z_2 symmetry and the neutrinos acquire masses at 1-loop level. This model has been extensively studied and some recent works on this can be seen in [11]. Supersymmetrizing this model could bring new features and it is done in [8]. In the supersymmetrization of the inert Higgs doublet model [8], the discreet symmetry is extended to $Z_2 \times Z_2'$. In this model, dark matter can be multi-partite [12] due to the presence of R-parity and the Z_2' symmetry. Some variations of this model are also presented in [13, 14]. In the model of [8], gauge coupling unification is possible by embedding it in a supersymmetric SU(5) structure [15]. The origin of the discrete symmetry $Z_2 \times Z_2'$, which is described above, is also explained by realizing it as a residual symmetry from a U(1) gauged symmetry [16].

In this work we consider the model of [8] and present the expression for neutrino masses, which arises from two 1-loop diagrams. We will demonstrate that neutrino masses are tiny in this model if either the neutrino Yukawa couplings are suppressed or some certain soft parameters of the scalar potential are fine-tuned. We consider the later case, in which the neutrino Yukawa couplings can be $\mathcal{O}(1)$, and they can drive LFV processes such as $\mu \to e\gamma$. In our work we assume flavor diagonal in the slepton mass matricies as well as in the A-terms of sleptons. Hence, in our model, lepton flavor violation is happening due to non-diagonal Yukawa couplings. Under the above mentioned scenario, we compute branching ratio for the decays $\ell_i \to \ell_j \gamma$. Among these decays, we show that

$\mu \to e\gamma$ can give stringent constraints on model parameters, especially on right-handed neutrino mass. Early calculations on $\mu \to e\gamma$ in a lepton number violating supersymmetric model can be seen in [17].

In the model of [8], apart from $\mu \to e\gamma$ there can also be an LFV decay of $\mu \to 3e$. In a Type-II seesaw mechanism for neutrino masses, the decay $\mu \to 3e$ can take place at tree level, due to the presence of triplet Higgs boson. In our model [8], there are no triplet Higgses, hence the decay $\mu \to 3e$ will take place at loop level. The current experimental upper limit on $Br(\mu \to 3e)$ is 1×10^{-12} [18], which is about two times larger than that of $Br(\mu \to e\gamma)$. So we can expect $Br(\mu \to e\gamma)$ to put somewhat tighter constraints on model parameters than that due to $Br(\mu \to 3e)$. Hence, in this work we focus on the computation of $Br(\mu \to e\gamma)$. It may happen that $Br(\mu \to 3e)$ and $Br(\mu \to e\gamma)$ may put some additional constraints on model parameters, but we study these in a separate work.

This paper is organized as follows. In the next section, we describe the model of [8]. In section 3, we present the expressions for neutrino masses and branching ratios for the decays $\ell_i \to \ell_j\gamma$. In section 4, we give neumerical results on neutrino masses and $\mu \to e\gamma$. We conclude in section 5.

2 The model

The model of Ref.[8] is an extension of minimal supersymmetric standard model (MSSM). The additional superfields of this model are as follows: (i) three right-handed neutrino fields, $\hat{N}_i$, $i = 1, 2, 3$, (ii) two electroweak doublets $\hat{\eta}_1 = (\hat{\eta}_1^0, \hat{\eta}_1^-)$, $\hat{\eta}_2 = (\hat{\eta}_2^+, \hat{\eta}_2^0)$, (iii) a singlet field $\hat{\chi}$. Under the electroweak gauge group $\mathrm{SU(2)}_L \times \mathrm{U(1)}_Y$, the charges of these additional superfields are given in Table 1. The model of Ref.[8] contains discrete

Field	$\hat{N}_i$	$\hat{\eta}_1$	$\hat{\eta}_2$	$\hat{\chi}$
$\mathrm{SU(2)}_L \times \mathrm{U(1)}_Y$	(1,0)	(2,-1/2)	(2,1/2)	(1,0)

Table 1: Charge assignments of additional superfields of the model under the electroweak gauge group.

symmetry $Z_2 \times Z_2'$, under which all the quark and Higgs superfields can be taken to be even. The leptons and the additional fields described above are charged non-trivially under this discrete symmetry [8]. The purpouse of this symmetry is to disallow the Yukawa term $\hat{L}_i \hat{H}_u \hat{N}_j$ in the superpotential of the model, and as a result the neutrino remains massless

at tree level. Here, $\hat{L}_i = (\hat{\nu}_i, \hat{\ell}_i)$, $i = 1, 2, 3$, are the lepton doublet superfields. The singlet charged lepton superfield is represented by $\hat{E}^c_i$, $i = 1, 2, 3$. We denote up- and down-type Higgs superfields as $\hat{H}_u$ and $\hat{H}_d$ respectively.

The superpotential of our model consisting of electroweak fields can be written as [8]

$$\begin{aligned} W &= (Y_E)_{ij}\hat{L}_i\hat{H}_d\hat{E}^c_j + (Y_\nu)_{ij}\hat{L}_i\hat{\eta}_2\hat{N}_j + \lambda_1\hat{H}_d\hat{\eta}_2\hat{\chi} + \lambda_2\hat{H}_u\hat{\eta}_1\hat{\chi} + \\ &\quad \mu\hat{H}_u\hat{H}_d + \mu_\eta\hat{\eta}_2\hat{\eta}_1 + \frac{1}{2}\mu_\chi\hat{\chi}\hat{\chi} + \frac{1}{2}M_{ij}\hat{N}_i\hat{N}_j \end{aligned} \tag{1}$$

Here, there is a summation over indices i, j which run from 1 to 3. The first and second terms in the above equation are Yukawa terms for charged leptons and neutrinos, respectively. But, as described before, $\hat{\eta}_2$ is odd under the discrete symmetry of the model and hence the scalar component of it does not acquire vacuum expectation value (vev) [8]. So neutrinos are still massless at tree level. Apart from the superpotential of Eq. (1), we should consider the scalar potential. The relavant terms in the scalar potential are given below.

$$\begin{aligned} V &= (m^2_L)_{ij}\tilde{L}^\dagger_i\tilde{L}_j + m^2_{\eta_1}\eta^\dagger_1\eta_1 + m^2_{\eta_2}\eta^\dagger_2\eta_2 + m^2_\chi\chi^*\chi + (m^2_N)_{ij}\tilde{N}^*_i\tilde{N}_j + \\ &\quad \Big[(AY_\nu)_{ij}\tilde{L}_i\eta_2\tilde{N}_j + (A\lambda)_1 H_d\eta_2\chi + (A\lambda)_2 H_u\eta_1\chi \\ &\quad + b_\eta\eta_2\eta_1 + \frac{1}{2}b_\chi\chi\chi + \frac{1}{2}(b_M)_{ij}\tilde{N}_i\tilde{N}_j + \text{c.c.}\Big]. \end{aligned} \tag{2}$$

As we have explained before that our motivation is to study LFV processes in the above described model. The LFV processes can be driven by charged sleptons. For instance, the off-diagonal elements of soft parameters, $(m^2_L)_{ij}$, can drive LFV processes. Similarly, we can write soft mass terms for singlet charged sleptons, $\tilde{E}_i, i = 1, 2, 3$, in the scalar potential. Also, there can exist A-terms connecting $\tilde{L}_i$ and $\tilde{E}_j$. The off-diagonal terms of the above mentioned soft terms can drive LFV processes, which actually exist in MSSM. Since our model [8] is an extension of MSSM, we are interested in LFV processes generated by the additional fields of this model. Hence, we assume that the off-diagonal terms of the soft terms, which are described above, are zero.

For simplicity, we assume that the parameters of the superpotential and scalar potential of our model are real. Then, by an orthogonal transformation among the neutrino superfields, $\hat{N}_i$, we can make the the following parameters to be diagonal, which are given below.

$$M_{ij} = M_i\delta_{ij}, \quad (m^2_N)_{ij} = (m^2_N)_i\delta_{ij}, \quad (b_M)_{ij} = (b_M)_i\delta_{ij} \tag{3}$$

By going to an appropriate basis of $\hat{L}_i$ and $\hat{E}_j$, we can get the Yukawa couplings for charged leptons to be diagonal. After doing this, we are left with no freedom and hence

the neutrino Yukawa couplings, $(Y_\nu)_{ij}$, can be non-diagonal. These non-diagonal Yukawa couplings can drive LFV processes such as $\ell_i \to \ell_j \gamma$. These LFV processes are driven at the 1-loop level, which we describe in the next section. As explained before, neutrinos also acquire masses at 1-loop level in this model [8]. To calculate these loop diagrams we need to know the mass eigenstates of the scalar and fermionic partners of the fields shown in Table 1, since these fields enter into the loop processes. Expressions for these mass eigenstates are given in Ref.[19]. However, our notations and conventions are different from that of Ref.[19]. Hence, for the sake of completeness we present them below.

The charged components of $\hat{\eta}_1, \hat{\eta}_2$ can be fermionic and scalar, which can be written as $(\tilde{\eta}_1^-, \tilde{\eta}_2^+)$ and (η_1^-, η_2^+), respectively. The two charged fermions represent chargino-type fields, whose mass is μ_η. Whereas, the charged scalars, in the basis $\Phi_+^{\rm T} = (\eta_2^+, \eta_1^{-*})$, will have a mass matrix which is given below.

$$\mathcal{L} \ni -\Phi_+^\dagger \begin{pmatrix} \mu_\eta^2 + m_{\eta_2}^2 + \frac{g^2-g'^2}{4} v^2 \cos(2\beta) & b_\eta \\ b_\eta & \mu_\eta^2 + m_{\eta_1}^2 - \frac{g^2-g'^2}{4} v^2 \cos(2\beta) \end{pmatrix} \Phi_+ \qquad (4)$$

Here, g, g' are the gauge couplings of $\mathrm{SU}(2)_L$ and $\mathrm{U}(1)_Y$, respectively. β is defined as $\tan\beta = \frac{v_2}{v_1} = \frac{\langle H_u^0 \rangle}{\langle H_d^0 \rangle}$ and $v^2 = v_1^2 + v_2^2$. We can diagonalize the above mass matrix by taking Φ_+ as

$$\Phi_+ = \begin{pmatrix} \cos\theta & -\sin\theta \\ \sin\theta & \cos\theta \end{pmatrix} \begin{pmatrix} \eta_{m2}^+ \\ \eta_{m1}^+ \end{pmatrix}, \quad \tan 2\theta = \frac{2 b_\eta}{m_{\eta_2}^2 - m_{\eta_1}^2 + (g^2 - g'^2) v^2 \cos(2\beta)/2} \qquad (5)$$

Here, η_{m1}^+ and η_{m2}^+ are mass eigenstates of the charged scalar fields and we denote their mass eigenvalues by m_{1+} and m_{2+}, respectively.

The neutral fermionic and scalar components of $\hat{\eta}_1, \hat{\eta}_2, \hat{\chi}$ can be written as $\Psi^{\rm T} = (\tilde{\eta}_1^0, \tilde{\eta}_2^0, \tilde{\chi})$ and $\Phi_0^{\rm T} = (\eta_1^0, \eta_2^0, \chi)$, respectively. The neutral fermionic fields will have a mixing mass matrix, which is given below.

$$\mathcal{L} \ni -\frac{1}{2} \Psi^{\rm T} M_\eta \Psi, \quad M_\eta = \begin{pmatrix} 0 & -\mu_\eta & -\lambda_2 v_2 \\ -\mu_\eta & 0 & \lambda_1 v_1 \\ -\lambda_2 v_2 & \lambda_1 v_1 & \mu_\chi \end{pmatrix} \qquad (6)$$

The above mixing matrix can be diagonalized by an orthogonal matrix as

$$U_\eta^{\rm T} M_\eta U_\eta = \mathrm{diag}(m_{\tilde{\eta}_1}, m_{\tilde{\eta}_2}, m_{\tilde{\eta}_3}) \qquad (7)$$

The neutral scalar fields of Φ_0 can be written as

$$\Phi_0 = \frac{1}{\sqrt{2}} \Phi_R + \frac{i}{\sqrt{2}} \Phi_I = \frac{1}{\sqrt{2}} \begin{pmatrix} \eta_{1R}^0 \\ \eta_{2R}^0 \\ \chi_R \end{pmatrix} + \frac{i}{\sqrt{2}} \begin{pmatrix} \eta_{1I}^0 \\ \eta_{2I}^0 \\ \chi_I \end{pmatrix} \qquad (8)$$

The mixing matrix among these fields can be written as

$$\mathcal{L} \ni -\frac{1}{2}\Phi_R^{\rm T} m_{\eta_R}^2 \Phi_R - \frac{1}{2}\Phi_I^{\rm T} m_{\eta_I}^2 \Phi_I \tag{9}$$

Here, the mixing matrices $m_{\eta_R}^2, m_{\eta_I}^2$ can be obtained from the following matrix

$$\begin{aligned}
m_\eta^2(\epsilon) &= \begin{pmatrix} m_{11}^2 & m_{12}^2 & m_{13}^2 \\ m_{12}^2 & m_{22}^2 & m_{23}^2 \\ m_{13}^2 & m_{23}^2 & m_{33}^2 \end{pmatrix}, \quad m_{11}^2 = \mu_\eta^2 + m_{\eta_1}^2 + \lambda_2^2 v_2^2 + \frac{g^2+g'^2}{4} v^2 \cos(2\beta), \\
m_{22}^2 &= \mu_\eta^2 + m_{\eta_2}^2 + \lambda_1^2 v_1^2 - \frac{g^2+g'^2}{4} v^2 \cos(2\beta), \quad m_{33}^2 = \mu_\chi^2 + m_\chi^2 + \lambda_1^2 v_1^2 + \lambda_2^2 v_2^2 + \epsilon b_\chi, \\
m_{12}^2 &= -\lambda_1\lambda_2 v_1 v_2 - \epsilon b_\eta, \quad m_{13}^2 = -\lambda_1 v_1 \mu_\eta - \lambda_2 v_2 \mu_\chi - \epsilon[(A\lambda)_2 v_2 - \mu\lambda_2 v_1] \\
m_{23}^2 &= \lambda_1 v_1 \mu_\chi + \lambda_2 v_2 \mu_\eta + \epsilon[(A\lambda)_1 v_1 - \mu\lambda_1 v_2]
\end{aligned} \tag{10}$$

Here, ϵ can take $+1$ or -1. We have $m_{\eta_R}^2 = m_\eta^2(+1)$ and $m_{\eta_I}^2 = m_\eta^2(-1)$. These two mixing mass matrices can be diagonalized by orthogonal matrices U_R and U_I, which are defined below.

$$U_R^{\rm T} m_{\eta_R}^2 U_R = {\rm diag}(m_{\eta_{R1}}^2, m_{\eta_{R2}}^2, m_{\eta_{R3}}^2), \quad U_I^{\rm T} m_{\eta_I}^2 U_I = {\rm diag}(m_{\eta_{I1}}^2, m_{\eta_{I2}}^2, m_{\eta_{I3}}^2) \tag{11}$$

At last, the fermionic and scalar components of right-handed neutrino superfields, $\hat{N}_i$, can be donted by N_i and $\tilde{N}_i$, respectively. The fermionic components have masses M_i. The scalar components can be decomposed into mass eigenstates as

$$\tilde{N}_i = \frac{1}{\sqrt{2}}\left(\tilde{N}_{Ri} + i\tilde{N}_{Ii}\right) \tag{12}$$

The mass-squares of $\tilde{N}_{Ri}$ and $\tilde{N}_{Ii}$, respectively, are given below.

$$m_{Ri}^2 = M_i^2 + (m_N^2)_i + (b_M)_i, \quad m_{Ii}^2 = M_i^2 + (m_N^2)_i - (b_M)_i \tag{13}$$

3 Neutrino masses and LFV processes

As described before that in the model of Ref.[8] neutrinos are massless at tree level due to the presence of the discrete symmetry $Z_2 \times Z_2'$. However, in this model neutrinos acquire masses at 1-loop level, whose diagrams are shown in Figure 1 [8]. After computing these 1-loop diagrams, we have found the following mass matrix for neutrinos.

$$\begin{aligned}
(m_\nu)_{ij} &= \sum_{k,l=1}^{3} \frac{(Y_\nu)_{ik}(Y_\nu)_{jk}}{16\pi^2} M_k \left[[U_R(2,l)]^2 \frac{m_{\eta_{Rl}}^2}{m_{\eta_{Rl}}^2 - M_k^2} \ln\frac{m_{\eta_{Rl}}^2}{M_k^2} - [U_I(2,l)]^2 \frac{m_{\eta_{Il}}^2}{m_{\eta_{Il}}^2 - M_k^2} \ln\frac{m_{\eta_{Il}}^2}{M_k^2} \right] \\
&\quad + \sum_{k,l=1}^{3} \frac{(Y_\nu)_{ik}(Y_\nu)_{jk}}{16\pi^2} [U_\eta(2,l)]^2 m_{\tilde{\eta}_l} \left[\frac{m_{Rk}^2}{m_{Rk}^2 - m_{\tilde{\eta}_l}^2} \ln\frac{m_{Rk}^2}{m_{\tilde{\eta}_l}^2} - \frac{m_{Ik}^2}{m_{Ik}^2 - m_{\tilde{\eta}_l}^2} \ln\frac{m_{Ik}^2}{m_{\tilde{\eta}_l}^2} \right]
\end{aligned} \tag{14}$$

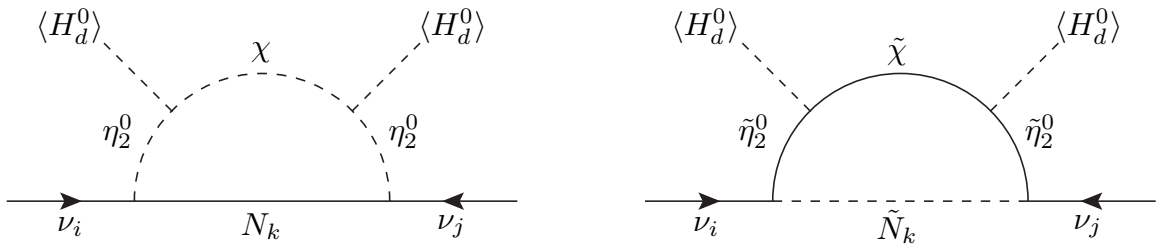

Figure 1: Radiative masses for neutrinos.

It is to be noticed that the first and second lines of the above equation arises from the left- and right-handed diagrams of Figure 1.

In our work we assume supersymmetry breaking to be around 1 TeV. Hence, we can take all the supersymmetric (SUSY) particle masses to be around few hundred GeV. With this assumption, we can estimate the neutrino Yukawa couplings by requiring that the neutrino mass scale to be around 0.1 eV [2]. With this requirement, we have found that $(Y_\nu)_{ij} \sim 10^{-5}$. Here there are six different Yukawa couplings, which need to be suppressed to $\mathcal{O}(10^{-5})$. This could be one possibility in this model in order to explain the correct magnitude for neutrino masses. However, in this case, since the Yukawa couplings are suppressed, LFV processes such as $\ell_i \to \ell_j \gamma$ would also be suppressed. These LFV processes will be searched in future experiments [20], hence it is worth to consider the case where these processes can have substancial contribution in this model. In otherwords, we have to look for a parameter region where we can have $(Y_\nu)_{ij} \sim \mathcal{O}(1)$.

From Eq. (14), it can observed that each diagram of Figure 1 contribute positive and negitive quantities to the neutrino mass matrix. Without suppressing Yukawa couplings, by fine-tuning the masses of SUSY particles, we may achieve partial cancellation between the positive and negative contributions of Eq. (14) and endup with tiny masses for neutrinos. To demonstrate this explicitly, using Eq. (13), we can notice that in the limit $(b_M)_i \to 0$ we get $m_{Ri}^2 - m_{Ii}^2 \to 0$, and hence the second line of Eq. (14) would give tiny contribution. The first line of Eq. (14) can give very small value in the following limiting process: $U_R(2,l) - U_I(2,l) \to 0$ and $m_{\eta_{Rl}} - m_{\eta_{Il}} \to 0$. To achieve this limiting process we have to make sure that the elements of the matrices $m_{\eta_R}^2$ and $m_{\eta_I}^2$ are close to each other. From the discussion around Eq. (10), we can observe that the elements of $m_{\eta_R}^2$ and $m_{\eta_I}^2$ can differ by quantities which are proportional to ϵ. These quantities depend on the following parameters: b_χ, b_η, $(A\lambda)_1$ and $(A\lambda)_2$. By taking the following limit: $(A\lambda)_1 - \lambda_1 \mu v_2/v_1 \to 0$, $(A\lambda)_2 - \lambda_2 \mu v_1/v_2 \to 0$, $b_\eta \to 0$, $b_\chi \to 0$, we can get tiny

contribution from the first line of Eq. (14). To sum up the above discussion, without suppressing the neutrino Yukawa couplings we can fine-tune the below seven paramters, in order to get very small neutrino masses in this model.

$$(b_M)_i, i = 1, 2, 3, \quad b_\eta, \quad b_\chi, \quad (A\lambda)_1, \quad (A\lambda)_2 \tag{15}$$

Apparently, the above parameters are SUSY breaking soft parameters of the scalar potential of this model. A study of neutrino masses depending on SUSY breaking soft parameters can be seen in [21].

In the previous paragraph we have argued that Majorana masses for neutrinos are vanishingly small when we fine tune certain soft parameters of the model. We can understand these features from symmetry arguments. For instance, when lepton number is conserved, neutrinos cannot have Majorana masses. For lepton number, we can propose a group $\mathrm{U}(1)_L$, under which the following fields are assigned the corresponding charges and the rest of the superfields are singlets.

$$\hat{L}_i \mapsto +1, \quad \hat{E}^c_i \mapsto -1, \quad \hat{N}_i \mapsto -1 \tag{16}$$

With the above mentioned charges, we can see that the last term in Eqs. (1) and (2) are forbidden. In fact, in the limit $M_i \to 0$ and $(b_M)_i \to 0$, the two diagrams of Figure 1 give zero masses to neutrinos. Hence, in order to get Majorana masses for neutrinos, we have softly broken the lepton number symmetry. Now, even if we have $M_i \neq 0$, we have described in the previous paragraph that the left-handed diagram of Figure 1 can still give vanishingly small masses by fine tuning some soft parameters. This suggests that apart from $\mathrm{U}(1)_L$ there can exist some additional symmetries. Suppose we set $(A\lambda)_1 v_1 - \lambda_1 \mu v_2 = 0$, $(A\lambda)_2 v_2 - \lambda_2 \mu v_1 = 0$. Then, as argued previously that the left-handed diagram of Figure 1 gives zero neutrino masses for $b_\eta \to 0$ and $b_\chi \to 0$, even if $M_i \neq 0$. This case can be understood by proposing additional symmetry $\mathrm{U}(1)_\eta$, under which the following fields have non-trivial charges and the rest of the fields are singlets.

$$\hat{L}_i \mapsto +1, \quad \hat{E}^c_i \mapsto -1, \quad \hat{\eta}_1 \mapsto -1, \quad \hat{\eta}_2 \mapsto -1, \quad \hat{\chi} \mapsto +1 \tag{17}$$

Using the above charges, we can notice that μ_η-, μ_χ-terms in Eq. (1) and b_η-, b_χ-terms in Eq. (2) are forbidden. Thus, the additional symmetry $\mathrm{U}(1)_\eta$ can forbid the Majorana masses for neutrinos in the left-handed diagram of Figure 1. Finally, one may ask how the relations $(A\lambda)_1 v_1 - \lambda_1 \mu v_2 = 0$, $(A\lambda)_2 v_2 - \lambda_2 \mu v_1 = 0$ can be satisfied. In these two relations, SUSY breaking soft masses are related to SUSY conserving mass μ. These

relations may be achieved my proposing certain symmetries in the mechansim for SUSY breaking, which is beyond the reach of our present work.

Previously, we have motivated a parameter region where the neutrino Yukawa couplings can be $\mathcal{O}(1)$. For these values of neutrino Yukawa couplings, LFV processes such as $\ell_i \to \ell_j \gamma$ can have substantical contribution in our model, and worth to compute them. The Feynman diagrams for $\ell_i \to \ell_j \gamma$ are given in Figure 2.

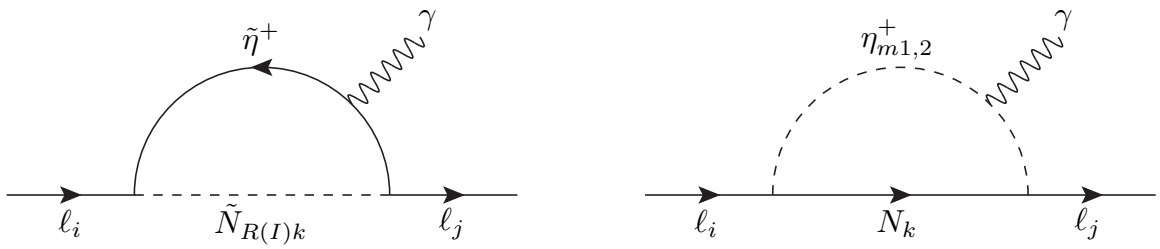

Figure 2: Lepton flavor violating decays of the form $\ell_i \to \ell_j \gamma$.

The general form of the amplitude for $\ell_i \to \ell_j \gamma$ is as follows.

$$\mathcal{M} = e\epsilon^*_\mu(q)\bar{u}_j(p-q)\left[A_L^{(ij)}\frac{1-\gamma_5}{2} + A_R^{(ij)}\frac{1+\gamma_5}{2}\right] i\sigma^{\mu\nu}q_\nu u_i(p) \tag{18}$$

It is to be noted that in the above equation, there is no summation over the indices i, j. The quantities $A_{L,R}^{(ij)}$ of the above equation can be found from the 1-loop diagrams of Figure 2, which we have given below.

$$\begin{aligned}
A_L^{(ij)} &= A^{(ij)} m_j, \quad A_R^{(ij)} = A^{(ij)} m_i, \\
A^{(ij)} &= \sum_{k=1}^{3} \frac{(Y_\nu)_{ik}(Y_\nu)_{jk}}{16\pi^2}\left\{\frac{1}{4\mu_\eta^2}\left[f_2(x_{Rk}) + f_2(x_{Ik})\right] - \left[\cos^2\theta \frac{f_2(x_{k2})}{2m_{2+}^2} + \sin^2\theta \frac{f_2(x_{k1})}{2m_{1+}^2}\right]\right\}, \\
x_{Rk} &= \frac{m_{Rk}^2}{\mu_\eta^2}, \quad x_{Ik} = \frac{m_{Ik}^2}{\mu_\eta^2}, \quad x_{k2} = \frac{M_k^2}{m_{2+}^2}, \quad x_{k1} = \frac{M_k^2}{m_{1+}^2}, \\
f_2(x) &= \frac{1}{(1-x)^4}\left[\frac{1}{6} - x + \frac{1}{2}x^2 + \frac{1}{3}x^3 - x^2\ln(x)\right].
\end{aligned} \tag{19}$$

From the above expressions, we can notice that in the curly brackets of $A^{(ij)}$, the first two and the last two terms are arising from the left- and right-handed diagrams of Figure 2, respectively. Moreover, there is a relative minus sign in the contribution from these two diagrams.

Among the various decays of the form $\ell_i \to \ell_j \gamma$, the upper bound on the branching ratio of $\mu \to e\gamma$ is found to be stringent [5]. Moreover, we have $Br(\mu \to e\bar{\nu}_e\nu_\mu) \approx 100\%$.

Using this and neglecting the electron mass, the branching ratio of $\mu \to e\gamma$ is found to be

$$Br(\mu \to e\gamma) = \frac{3\alpha}{16\pi G_F^2}\left|\sum_{k=1}^{3}(Y_\nu)_{1k}(Y_\nu)_{2k}\times \left\{\frac{1}{4\mu_\eta^2}\left[f_2(x_{Rk})+f_2(x_{Ik})\right]-\left[\cos^2\theta\frac{f_2(x_{k2})}{2m_{2+}^2}+\sin^2\theta\frac{f_2(x_{k1})}{2m_{1+}^2}\right]\right\}\right|^2 \quad (20)$$

Here, $\alpha = \frac{e^2}{4\pi}$ and G_F is the Fermi constant.

Here we compare our work with that of Ref.[14]. The model in [14] is similar to that of [8]. But, in [14], a theory at a high scale with an anomalous $U(1)_X$ symmetry is assumed. The $U(1)_X$ symmetry breaks into Z_2 symmetry at a low scale. Due to these differences, there exists three 1-loop diagrams for neutrinos in [14], whereas only two diagrams generate neutrino masses in [8]. The diagrams for the LFV processes of $\ell_i \to \ell_j\gamma$ in [14] is similar to the diagrams given in this paper (see Figure 2). But the expression for $Br(\mu \to e\gamma)$, which is given in Eq. (20), is found to be different from that in [14]. We hope that these differences might have arised since the model in [14] has different origin from that of [8].

Although the main motivation of this paper is to study the correlation between neutrino masses and $Br(\mu \to e\gamma)$, below we mention about muon $g-2$ in our model. It is known that the theoretical [22] and experimental [23] values of muon $g-2$ differ by about 3σ deviation. However, there are hadronic uncertainities to muon $g-2$, which need to be improved [22]. Hence, the above mentioned result is still an indication for new physics signal. In our model [8], muon $g-2$ get contributions from MSSM fields [24] as well as from additional fields, which are shown in Table 1. The contribution from MSSM fields can fit the 3σ discrepancy of muon $g-2$[1]. Hence, in our model [8], it is interesting to know how large would be the contribution from the additional fields of this model. The contribution from these additional fields can be found from the amplitude of Eq. (18), which is given below.

$$\Delta a_\mu = \frac{m_\mu^2}{16\pi^2}\sum_{k=1}^{3}\left[(Y_\nu)_{2k}\right]^2\left\{\frac{1}{2\mu_\eta^2}\left[f_2(x_{Rk})+f_2(x_{Ik})\right]-\left[\cos^2\theta\frac{f_2(x_{k2})}{m_{2+}^2}+\sin^2\theta\frac{f_2(x_{k1})}{m_{1+}^2}\right]\right\} \quad (21)$$

Here, m_μ is mass of the muon.

[1]In Ref.[25], the discrepancy in muon $g-2$ is fitted in a supersymmetric model, where the contribution is actually from the MSSM fields.

4 Analysis and results

As described in section 1 that our motivation is to study the correlation between neutrino masses and $Br(\mu \to e\gamma)$. We have given expression for neutrino masses in Eq. (14). We have explained in the previous section that to explain neutrino mass scale of 0.1 eV, we can make neutrino Yukawa couplings to be about $\mathcal{O}(1)$, but we need to fine-tune certain SUSY breaking soft parameters which are given in Eq. (15). We consider this case, since for unsuppressed neutrino Yukawa couplings, $Br(\mu \to e\gamma)$ can have maximum values. As mentioned before, experiments have put the following upper bound: $Br(\mu \to e\gamma) < 5.7 \times 10^{-13}$ [5]. Hence, for the above mentioned parameter space, where neutrino Yukawa couplings are unsuppressed, we compute $Br(\mu \to e\gamma)$ by fitting neutrino masses. We check if the computed values for $Br(\mu \to e\gamma)$ satisfy the experimental bound [5].

Before we compute $Br(\mu \to e\gamma)$, we first need to ensure that the neutrino Yukawa couplings can be unsuppressed in our model. We can calculate these Yukawa couplings from Eq. (14) by fitting to the neutrino oscillation data. The neutrino mass matrix of Eq. (14) is related to neutrino mass eigenvalues through the following relation.

$$m_\nu = U^*_{\rm PMNS} {\rm diag}(m_1, m_2, m_3) U^\dagger_{\rm PMNS}. \tag{22}$$

Here, $m_{1,2,3}$ are the mass eigenvalues of neutrinos and $U_{\rm PMNS}$ is the Pontecorvo-Maki-Nakagawa-Sakata matrix. The matrix $U_{\rm PMNS}$ depends on three mixing angles $(\theta_{12}, \theta_{23}, \theta_{13})$ and Dirac CP-violating phase, $\delta_{\rm CP}$. In the above equation there is a possibility of Majarona phases, which we have taken to be zero, for simplicity. We have parametrized $U_{\rm PMNS}$ in terms of mixing angles and $\delta_{\rm CP}$ as it is given in [7].

By fitting to various neutrino oscillation data, we haven known solar and atmospheric neutrino mass-square differences and also about the neutrino mixing angles [26]. In the case of normal hierarchy (NH) of neutrino masses, we have taken the mass-square differences as

$$\Delta m^2_{21} = m_2^2 - m_1^2 = 7.6 \times 10^{-5}\ {\rm eV}^2, \quad |\Delta m^2_{31}| = |m_3^2 - m_1^2| = 2.48 \times 10^{-3}\ {\rm eV}^2 \tag{23}$$

In the case of inverted hierarchy (IH) of neutrino masses, the value of Δm^2_{21} remains the same as mentioned above, but, $|\Delta m^2_{31}| = 2.38 \times 10^{-3}\ {\rm eV}^2$. In this work, the neutrino mixing angles and CP-violating phase are chosen to be

$$\sin\theta_{12} = \frac{1}{\sqrt{3}}, \quad \sin\theta_{23} = \frac{1}{\sqrt{2}}, \quad \sin\theta_{13} = 0.15, \quad \delta_{\rm CP} = 0 \tag{24}$$

The above mentioned neutrino mass-square differences, mixing angles and CP-violating phase are consistent with the fitted values in [26]. From the mass-square differences, we

can estimate neutrino mass eigenvalues which are given below for the cases of NH and IH, respectively.

$$m_1 = 0, \quad m_2 = \sqrt{\Delta m^2_{21}}, \quad m_3 = \sqrt{|\Delta m^2_{31}|} \tag{25}$$

$$m_3 = 0, \quad m_1 = \sqrt{|\Delta m^2_{31}|}, \quad m_2 = \sqrt{\Delta m^2_{21} + m^2_1} \tag{26}$$

In the previous paragraph, we have mentioned neumerical values of neutrino mass eigenvalues, mixing angles and CP-violating phase. By plugging these values in Eq. (22), we can compute the elements of the matrix m_ν, which are related to neutrino Yukawa couplings and SUSY parameters through Eq. (14). Using Eq. (14), we can calculate neutrino Yukawa couplings, in order to satisfy neutrino oscillation data. This calculation procedure would become simplified if we assume degenerate masses for right-handed neutrinos and right-handed sneutrinos. For $i = 1, 2, 3$, we assume the following:

$$M_i = M, \quad (m^2_N)_i = m^2_N, \quad (b_M)_i = b_M \tag{27}$$

Under the above assumption, all the three right-handed neutrinos have mass M. The corresponding sneutrinos have real and imaginary components (see Eq. (12)), whose masses would be

$$m^2_R = M^2 + m^2_N + b_M, \quad m^2_I = M^2 + m^2_N - b_M \tag{28}$$

Under the above mentioned assumption, the neutrino mass matrix of Eq. (14) will be simplified to

$$\begin{aligned}(m_\nu)_{ij} &= \frac{S_{ij}}{16\pi^2}\sum_{l=1}^{3}\left\{M\left[[U_R(2,l)]^2\frac{m^2_{\eta_{Rl}}}{m^2_{\eta_{Rl}} - M^2}\ln\frac{m^2_{\eta_{Rl}}}{M^2} - [U_I(2,l)]^2\frac{m^2_{\eta_{Il}}}{m^2_{\eta_{Il}} - M^2}\ln\frac{m^2_{\eta_{Il}}}{M^2}\right] + \right. \\ &\left. [U_\eta(2,l)]^2 m_{\tilde{\eta}_l}\left[\frac{m^2_R}{m^2_R - m^2_{\tilde{\eta}_l}}\ln\frac{m^2_R}{m^2_{\tilde{\eta}_l}} - \frac{m^2_I}{m^2_I - m^2_{\tilde{\eta}_l}}\ln\frac{m^2_I}{m^2_{\tilde{\eta}_l}}\right]\right\}, \end{aligned} \tag{29}$$

$$S_{ij} = \sum_{k=1}^{3}(Y_\nu)_{ik}(Y_\nu)_{jk} \tag{30}$$

The elements S_{ij} are expressed quadratic in neutrino Yukawa couplings. From the above relation we can see that for certain values of SUSY parameters, S_{ij} can be calculated from $(m_\nu)_{ij}$. Using the above mentioned assumption of degenerate masses for right-handed neutrinos and right-handed sneutrinos, we can see that Eqs. (20) & (21) would give us $Br(\mu \to e\gamma) \propto S^2_{21}$ and $\Delta a_\mu \propto S_{22}$.

In our model, there are plenty of SUSY parameters, and we need to fix some of them to simplify our analysis. In our analysis, we have chosen the following SUSY parameters as follows.

$$\mu_\chi = 600 \text{ GeV}, \quad m_{\eta_1} = 400 \text{ GeV}, \quad m_{\eta_2} = 500 \text{ GeV}, \quad m_\chi = 600 \text{ GeV},$$
$$m_N = 700 \text{ GeV}, \quad \lambda_1 = 0.5, \quad \lambda_2 = 0.6, \quad \tan\beta = 10 \tag{31}$$

We have varied the parameters μ_η and M, freely. In the previous section, we have explained that we need to fine-tune the parameters of Eq. (15) in order to get small neutrino masses. Among these parameters, we take $(A\lambda)_1 = \lambda_1 \mu v_2/v_1$ and $(A\lambda)_2 = \lambda_2 \mu v_1/v_2$. The other parameters of Eq. (15), without loss of generality, are taken to be degenerate, which are given below.

$$b_M = b_\eta = b_\chi = b_{\text{susy}} \tag{32}$$

We have explained before that we have assumed degenerate masses for right-handed neutrinos and right-handed sneutrinos. Under this assumption, the information of neutrino Yukawa couplings is contained in the quantities S_{ij}. Hence, it is worth to plot these quantities to know about neutrino Yukawa couplings. In Figure 3, for the case of NH, we have plotted S_{21} and S_{22} versus right-handed neutrino mass, M, for $\mu_\eta = 1$ TeV. The plots

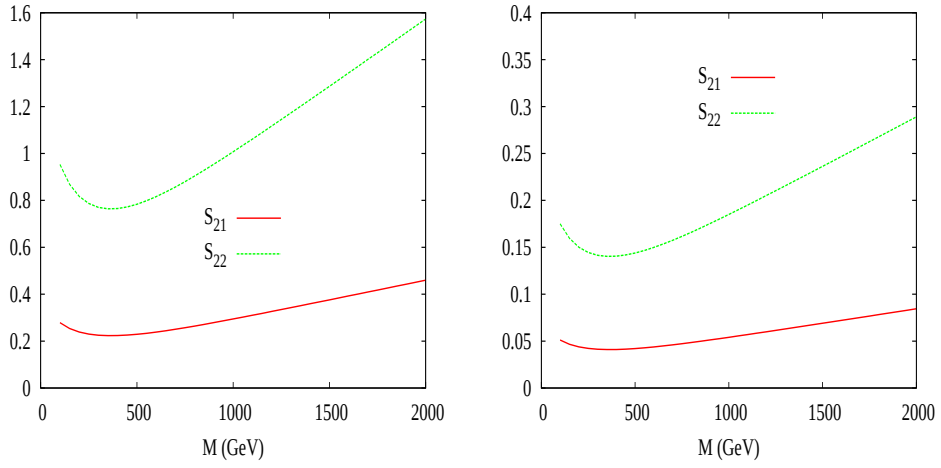

Figure 3: The quantities S_{21}, S_{22} are plotted against right-handed neutrino mass for $\mu_\eta = 1$ TeV, in the case of NH. In the left- and right-handed plots, b_{susy} is taken to be $(3\times10^{-2})^2$ GeV^2 and $(7\times10^{-2})^2$ GeV^2, respectively.

of Figure 3 indicate that S_{22} and S_{21} are around $\mathcal{O}(1)$. Since these quantities are sum of squares of neutrino Yukawa couplings (see, Eq. (30)), we can expect that the neutrino

Yukawa couplings should be in the range of $\mathcal{O}(1)$. We have not plotted the values of S_{11}, S_{31}, etc in Figure 3, but we have found that these will also be around $\mathcal{O}(1)$. We have plotted S_{21} and S_{22} in Figure 3, since these two determine $Br(\mu \to e\gamma)$ and Δa_μ.

From the plots of Figure 3, we can notice that the values of S_{22} are higher than that of S_{21}. This fact follows from Eq. (29), where we can see that S_{ij} are proportional to $(m_\nu)_{ij}$, which are determined by neutrino oscillation parameters. In the case of NH, we have seen that $(m_\nu)_{22}$ is greater than $(m_\nu)_{21}$ by a factor of 3.4, hence S_{22} is always found to be larger than S_{21}. It is clear from the plots of Figure 3 that by increasing $b_{\rm susy}$, S_{21} and S_{22} would decrease. Again, this feature can be understood from Eq. (29). As explained in the previous section, the square brackets of Eq. (29) would tend to zero in the limit $b_{\rm susy} \to 0$. So for large value of $b_{\rm susy}$ there will be less partial cancellation in the square brackets, and hence S_{21} and S_{22} would decrease. In both the plots of Figure 3, it is found that the values of S_{21} and S_{22} initially decreases with M, goes to a minima and then increases. The shape of these curves can be understood by applying the approximation of $\frac{b_{\rm susy}}{M^2} \ll 1$ in Eq. (29). In the limit $b_{\rm susy} \to 0$, we can take

$$m^2_{\eta_{Rl}} = m^2_{\eta_l}(1+\delta_{Rl}), \quad m^2_{\eta_{Il}} = m^2_{\eta_l}(1+\delta_{Il}), \quad U_R(2,l) \approx U_I(2,l) = U_0(2,l) \tag{33}$$

Here, $\delta_{Rl}, \delta_{Il} \ll 1$. Using the above mentioned approximations in Eq. (29), we get

$$\begin{aligned}(m_\nu)_{ij} \;=\; & \frac{S_{ij}}{16\pi^2}\sum_{l=1}^{3}\Bigg\{[U_0(2,l)]^2(\delta_{Rl}-\delta_{Il})M\frac{m^2_{\eta_l}}{m^2_{\eta_l}-M^2}\left[1-\frac{M^2}{m^2_{\eta_l}-M^2}\ln\frac{m^2_{\eta_l}}{M^2}\right]+ \\ & [U_\eta(2,l)]^2 m_{\tilde{\eta}_l}\frac{2b_{\rm susy}}{M^2+m^2_N-m^2_{\tilde{\eta}_l}}\left[1-\frac{m^2_{\tilde{\eta}_l}}{M^2+m^2_N-m^2_{\tilde{\eta}_l}}\ln\frac{M^2+m^2_N}{m^2_{\tilde{\eta}_l}}\right]\Bigg\}\end{aligned} \tag{34}$$

In the summation of the above equation, the first and second lines arise due to left- and right-handed diagrams of Figure 1. From the above equation, we can understand that the contribution from the first line increases, reaches a maximum, and then decreases with M. Whereas, the contribution from the second line of the above equation decreases monotonically with M. It is this functional dependence on M that determine the shape of the lines in Figure 3. Physically, in the limit $b_{\rm susy} \to 0$, the above description suggests that the right-handed diagram of Figure 1 is significant only for very low values of M. For other values of M, the left-handed diagram of Figure 1 gives dominant contribution to neutrino masses. One remark about the plots in Figure 3 is that we have fixed $\mu_\eta = 1$ TeV in these figures. We have varied μ_η from 500 GeV to 1.5 TeV and have found that the plots in Figure 3 would change quantitatively, but qualitative features would remain same. Also, the plots in Figure 3 are for the case of NH. Again, these plots can change

quantitatively, if not qualitatively, for the case of IH. For this reason, below we present our results on $Br(\mu \to e\gamma)$ and muon $g-2$ for the case of NH only.

As described before that our motivation is to compute $Br(\mu \to e\gamma)$ in the model of [8]. In Figure 3 we have shown that the neutrino Yukawa couplings in this model can be $\mathcal{O}(1)$, and for these values of Yukawa couplings, $Br(\mu \to e\gamma)$ is unsuppressed. In the parameter space where neutrino Yukawa couplings are unsuppressed, we have plotted $Br(\mu \to e\gamma)$ as a function of right-handed neutrino mass. These plots are shown in Figure 4, where we have also varied μ_η from 500 GeV to 1.5 TeV. The horizontal line in these plots indicate

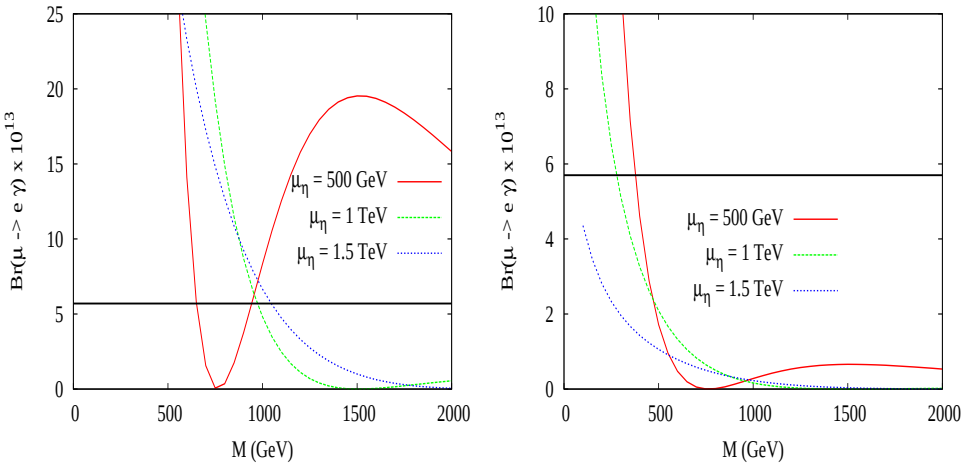

Figure 4: $Br(\mu \to e\gamma)$ is plotted against right-handed neutrino mass for different values of μ_η. In the left- and right-handed plots, $b_{\rm susy}$ has been taken as $(3 \times 10^{-2})^2$ GeV^2 and $(7 \times 10^{-2})^2$ GeV^2, respectively. The horizontal line indicates the current upper bound on $Br(\mu \to e\gamma)$.

the current upper bound of $Br(\mu \to e\gamma) < 5.7 \times 10^{-13}$. This upper bound would impose lower bound on the right-handed neutrino mass, as can be seen in the plots of Figure 4. In the left-handed plot of Figure 4, for $\mu_\eta = 500$ GeV, the right-handed neutrino mass is allowed to be between about 650 to 950 GeV. In the same plot, for $\mu_\eta = 1$ or 1.5 TeV, the right-handed neutrino mass has a lower bound of about 1 TeV. In the right-handed plot of Figure 4, the lower bound on right-handed neutrino mass is within 500 GeV, even for a low value of $\mu_\eta = 500$ GeV.

The lower bounds on the right-handed neutrino mass, M, are severe in the left-handed plot of Figure 4. The reason is that for low value of $b_{\rm susy}$, S_{21} would be high, and hence $Br(\mu \to e\gamma)$ would be large. From Figure 4, we can observe that $Br(\mu \to e\gamma)$ initially decreases with M, goes to a minimum and then increases. For instance, in the left-

handed plot of Figure 4, for $\mu_\eta = 500$ GeV, $Br(\mu \to e\gamma)$ goes to a minimum around $M = 750$ GeV, and then it will have a local maxima around $M = 1.5$ TeV. The reason for $Br(\mu \to e\gamma)$ to initially decrease with M is due to the fact that the decay $\mu \to e\gamma$ is driven by right-handed neutrinos and right-handed sneutrinos, as given in Figure 2. The masses of right-handed neutrinos and right-handed sneutrinos are proportional to M, and hence $Br(\mu \to e\gamma)$ would be suppressed with increasing M. After that, at a certain value of M, $Br(\mu \to e\gamma)$ would tend to become zero. The reason for this is that the sum of the two diagrams of Figure 2 gives a relative minus sign to the contribution of $Br(\mu \to e\gamma)$, which is given in Eq. (20). Hence, for a particular value of M, the contributions from both the two diagrams of Figure 2 cancel out and give a minimum for $Br(\mu \to e\gamma)$. Also, $Br(\mu \to e\gamma)$ can go to zero asymptotically when $M \to \infty$, since in this limit the masses of right-handed neutrinos and right-handed sneutrinos would become infinitely large and suppress $Br(\mu \to e\gamma)$. Hence, $Br(\mu \to e\gamma)$ has two zeros on the M-axis. As $Br(\mu \to e\gamma)$ is a continous function of M and is always a positive quantity, it is having a local maxima between the two zeros on the M-axis.

In the previous section we have described about muon $g-2$. In Eq. (21), we have given the contribution due to additional fields (see Table 1) of our model to the muon $g-2$. Apart from this contribution, MSSM fields of our model also contribute to muon $g-2$ [24], and it is known that this contribution fits the 3σ discrepancy of muon $g-2$. Hence, it is interesting to know if the additional contribution of Eq. (21) could be as large as that of MSSM contribution to muon $g-2$. In Figure 5, we have plotted the contribution of Eq. (21). In the plots of Figure 5, we have chosen the parameter region such that the neutrino oscillation data is fitted. From the plots of Figure 5, we can see that for low values of M, Δa_μ can be negative and it becomes positive after certain large value of M. From these plots we can notice that the overall magnitude of Δa_μ is not more than about 10^{-12}. This contribution is atleast two orders smaller than the estimated discrepancy of muon $g-2$, which is $(29 \pm 9) \times 10^{-10}$ [22]. From this we can conclude that the additional contribution to muon $g-2$ in our model, *i.e.* Eq. (21), is insignificant compared to the MSSM contribution to muon $g-2$.

5 Conclusions

We have worked in a supersymmetric model where neutrino masses arise at 1-loop level [8]. We have computed these loop diagrams and obtained expressions for neutrino masses. We have identified a parameter region of this model, where the neutrino osicllation data

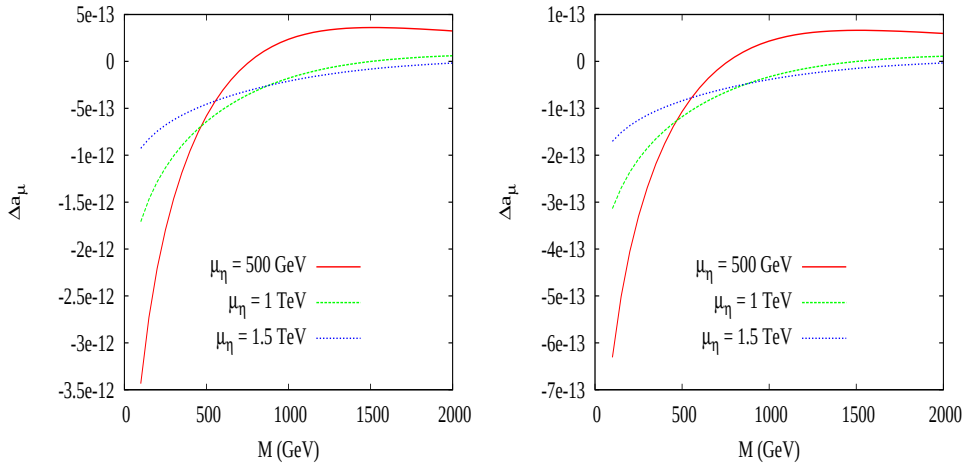

Figure 5: Δa_μ is plotted against right-handed neutrino mass for different values of μ_η. In the left- and right-handed plots, $b_{\rm susy}$ has been taken as $(3 \times 10^{-2})^2$ GeV^2 and $(7 \times 10^{-2})^2$ GeV^2, respectively.

can be fitted without the need of suppressing the neutrino Yukawa couplings. In our parameter region, the SUSY breaking soft parameters such as b_M, b_η, b_χ, $(A\lambda)_1$, $(A\lambda)_2$ need to be fine-tuned. In this parameter region, branching fraction of $\mu \to e\gamma$ can be unsuppressed, and hence, we have computed $Br(\mu \to e\gamma)$. We have shown that the current upper bound on $Br(\mu \to e\gamma)$ can put lower bounds on the mass of right-handed neutrino field. Depending on the parameteric choice, we have found that this lower bound can be about 1 TeV. We have also computed the contribution to muon $g-2$ arising from additional fields of this model, which are given in Table 1. We have shown that, in the region where neutrino oscillation data is fitted, the above mentioned contribution is two orders smaller than the discrepancy in muon $g-2$.

References

[1] C. Quigg, arXiv:hep-ph/0404228;
J. Ellis, Nucl. Phys. A **827** (2009) 187C [arXiv:0902.0357 [hep-ph]].

[2] R. N. Mohapatra, arXiv:hep-ph/0211252;
Y. Grossman, arXiv:hep-ph/0305245;
A. Strumia and F. Vissani, arXiv:hep-ph/0606054.

[3] H. P. Nilles, Phys. Rept. **110**, (1984) 1;
H. E. Haber and G. L. Kane, Phys. Rept. **117**, (1985) 75;
S. P. Martin, arXiv:hep-ph/9709356;
M. Drees, R. Godbole and P. Roy, Theory and Phenomenology of Sparticles, (World Scientific, 2004);
P. Binetruy, Supersymmetry (Oxford University Press, 2006);
H. Baer and X. Tata, Weak Scale Supersymmetry: From Superfields to Scattering Events, (Cambridge University Press, 2006).

[4] T. Mori, eConf C **060409**, (2006) 034 [hep-ex/0605116];
J. M. Yang, Int. J. Mod. Phys. A **23**, (2008) 3343 (2008) [arXiv:0801.0210 [hep-ph]];
A. J. Buras, Acta Phys. Polon. Supp. **3**, (2010) 7 (2010) [arXiv:0910.1481 [hep-ph]];
Y. Nir, CERN Yellow Report CERN-2010-001, 279-314 [arXiv:1010.2666 [hep-ph]].

[5] J. Adam *et al.* (MEG Collaboration), Phys. Rev. Lett. **110** (2013) 201801.

[6] B. Aubert *et al.* (BaBar Collaboration), Phys. Rev. Lett. **104** (2010) 021802.

[7] K.A. Olive *et al.* (Particle Data Group), Chin. Phys. C **38** (2014) 090001.

[8] E. Ma, Annales Fond. Broglie **31** (2006) 285, [arXiv:hep-ph/0607142].

[9] E. Ma, Phys. Rev. D **73** (2006) 077301.

[10] R. Barbieri, L.J. Hall and V.S. Rychkov, Phys. Rev. D**74** (2006) 015007.

[11] A. Arhrib, R. Benbrik, J.E. Falaki and A. Jueid, [arXiv:1507.03630];
A.D. Plascencia, JHEP 1509 (2015) 026;
S. Kashiwase and D. Suematsu, Phys. Lett. B**749** (2015) 603.

[12] Q.-H. Cao, E. Ma, Jose Wudka and C.-P. Yuan, arXiv:0711.3881.

[13] H. Fukuoka, J. Kubo and D. Suematsu, Phys. Lett. B **678** (2009) 401;
D. Suematsu, T. Toma and T. Yoshida, Int. J. Mod. Phys. A**25** (2010) 4033.

[14] D. Suematsu and T. Toma, Nucl. Phys. B**847** (2011) 567.

[15] E. Ma, Phys. Lett. B**659** (2008) 885.

[16] E. Ma, Mod. Phys. Lett. A**23** (2008) 721.

[17] I-H. Lee, Phys. Lett. B**138** (1984) 121; Nucl. Phys. B**246** (1984) 120.

[18] U. Bellgardt *et al.* (SINDRUM Collaboration), Nucl. Phys. B**299** (1988) 1.

[19] M. Aoki, J. Kubo, T. Okawa and H. Takano, Phys. Lett. B**707** (2012) 107.

[20] A.M. Baldini *et al.*, arXiv:1301.7225;
T. Aushev *et al.*, arXiv:1002.5012.

[21] A.J.R. Figueiredo, Eur. Phys. J. C**75** (2015) 3, 99.

[22] F. Jegerlehner and A. Nyffeler, Phys. Rept. **477** (2009) 1;
T. Blum, A. Denig, I. Logashenko, E. de Rafael, B. Lee Roberts, T. Teubner and G. Venanzoni, arXiv:1311.2198.

[23] G.W. Bennett *et al.* (Muon g-2 Collaboration), Phys. Rev. D**73** (2006) 072003.

[24] T. Moroi, Phys. Rev. D**53** (1996) 6565 [Erratum-ibid. D**56** (1997) 4424];
S.P. Martin and J.D. Wells, Phys. Rev. D**64** (2001) 035003.

[25] R.S. Hundi, Phys. Rev. D**83** (2011) 115019.

[26] D.V. Forero, M. Tortola and J.W.F. Valle, Phys. Rev. D**90** (2014) 093006.